NEOPLASIA
www.neoplasia.com

Volume 35 Number xxx Month 2023 pp. 100845

Original Research

HDAC6 promotes aggressive development of liver cancer by improving egfr mRNA stability

Hong-Ying Dai [a,b]; Long-Sen Chang [a]; Sheau-Fang Yang [c]; Shen-Nien Wang [d]; Shu-Jem Su [e]; Yao-Tsung Yeh [b,e,*]

[a] Institute of Biomedical Sciences, National Sun Yat-Sen University, Kaohsiung, No. 70, Lienhai Rd., Kaohsiung City, 80424, Taiwan
[b] Aging and Disease Prevention Research Center, Fooyin University, Kaohsiung, No.151, Jinxue Rd., Daliao Dist., Kaohsiung City, 83102, Taiwan
[c] Department of Pathology, Faculty of Medicine, College of Medicine, Kaohsiung Medical University, Kaohsiung, No.100, Shih-Chuan 1st Rd., Sanmin Dist., Kaohsiung City, 80708, Taiwan
[d] Department of Surgery, Faculty of Medicine, Kaohsiung Medical University, Kaohsiung, No.100, Shih-Chuan 1st Rd., Sanmin Dist., Kaohsiung City, 80708, Taiwan
[e] Department of Medical Laboratory Sciences and Biotechnology, Fooyin University, Kaohsiung, No.151, Jinxue Rd., Daliao Dist., Kaohsiung City, 83102, Taiwan

Keywords: HDAC6, EGFR, liver cancer, HuR, mRNA stability

Introduction

Alterations of histone deacetylases (HDACs) have been found in various types of cancers [1]. Among HDAC family members, HDAC6 is the only HDAC that possesses two functional deacetylase domains and participates in multiple functions including autophagy, mRNA stability, co-repression of transcription, etc. [2,3]. HDAC6 is able to promote oncogenic transformation [4], and has been also found to increase cell migration and invasion in liver cancer cells [5,6]. Controversially, in clinic, HDAC6 suppresses neoplastic and antiphagocytic behaviors in hepatocellular carcinoma (HCC) [7] through activation of c-Jun NH2-terminal kinase-mediated beclin 1-dependent autophagic cell death [5,8]. In general, HDAC6 is mainly localized in the cytoplasm and is regarded as a tubulin-specific deacetylase [9,10]. HDAC6 exerts different functions in the nucleus. For example, HDAC6 enters the nucleus and interacts with survivin to regulate its acetylation status and to promote its nuclear exit, thus blocking programmed cell death [11]. In contrast, our previous study showed that nuclear HDAC6 directly bound to and deacetylated NF-κB to inhibit the downregulation of matrix metalloproteinase 2 (MMP2), preventing the invasiveness of lung cancer cells [12]. The impacts of HDAC6 on liver cancer as well as related mechanisms remain mostly unclear and require further investigations.

An RNA-binding protein is a type of post-transcriptional regulatory protein that can bind to RNA and change the fate and function of the bound RNAs [13]. Human antigen R (HuR) can bind to the adenine-uracil-rich elements (ARE) at the 3′UTR of the target mRNA molecule and further regulates a variety of biological processes [14]. Sharma et al. showed that HuR can stabilize the *egfr* transcript [15]. More intriguingly, HDAC6 is reported to regulate the stability of *erbb2* mRNA, one of the EGFR members, by interacting with HuR [16]. A ligand-dependent degradation of EGFR protein also appeared to rely on HDAC6 [17,18], while HDAC6 can associate with the endosomal compartments and further modulate endocytic trafficking of ligand-bound EGFR proteins [19]. Nevertheless, the mechanism underlying the interplay between HDAC6 and ligand-unbound EGFR remains undetermined. EGFR overexpression and related signaling pathway are closely associated with aggressive behaviors [20,21]. Besides, EGFR is frequently overexpressed in HCC patients [22,23] and related cell lines [24]. Tyrosine kinase inhibitors (TKIs) is found to be effective in treating advanced HCC [25]. However, constitutive EGFR activation is remained as a potential determinant of primary resistance to sorafenib [26] and lenvatinib [27].

In this study, we investigated the prognostic value of subcellular localization patterns of HDAC6 in liver cancer. Furthermore, we provide evidence that one of the mechanisms underlying the roles of HDAC6 in liver cancer might act by stabilizing *egfr* transcripts and by activating related downstream signaling. The HDAC6-EGFR axis may represent a rational therapeutic target in the development of advanced liver cancer.

Abbreviations: HDAC6, Histone deacetylase 6; MTT, 3-(4,5-Dimethylthiazol-2-yl)-2,5-diphenyltetrazolium bromide; PCR, Polymerase chain reaction; IF, Immunofluorescence; IB, Immunoblotting; IP, Immunoprecipitation; RNP-IP, Ribonucleoprotein immunoprecipitation; EGFR, Epidermal growth factor receptor; HCC, hepatocellular carcinoma; HuR, Human antigen R; 3'UTR, 3' untranslated region.

* Corresponding author at: Aging and Disease Prevention Research Center, Department of Medical Laboratory Sciences and Biotechnology, Fooyin University, No.151, Jinxue Rd., Daliao Dist., Kaohsiung City, 83102, Taiwan.
E-mail address: glycosamine@yahoo.com.tw (Y.-T. Yeh).
Received 8 June 2022; accepted 12 October 2022

https://doi.org/10.1016/j.neo.2022.100845

Materials and Methods

Liver cancer tissue microarray (TMA)

The use of all tissues was approved by the Kaohsiung Medical University Hospital, with IRB approval (KMUHIRB-E(I)20160084). One hundred and twenty-two liver cancer specimens were purchased from SuperBioChips Laboratories (Seoul, South Korea; TMA catalog number CS). Clinicopathological information can be obtained from the website (http://www.tissue-array.com). The tissue slides stained with hematoxylin and eosin were made available online by the manufacturers (Superbiochips Laboratories, Seoul, Korea). The pathologic staging, and histologic findings were determined according to the American Joint Committee on Cancer (AJCC) criteria [28].

Immunohistochemistry and image processing

The detailed protocol for immunohistochemistry (IHC) was performed as previously described [29,30]. Briefly, the tissue microarray was dewaxed and rehydrated. After antigen retrieval and blocking with 3% H_2O_2 and 10% normal goat serum, the slides were then incubated with rabbit polyclonal antibodies against HDAC6 (H300) diluted 1:100 (sc-11420, Santa Cruz Biotechnology Inc., CA, USA) at 4 °C for 24 h. UltraVision Quanto Detection System horseradish peroxidase (HRP) Polymer (Thermo Fisher Scientific, Waltham, MA, USA), and DAB Quanto (Thermo Fisher Scientific, Waltham, MA, USA) were applied for staining, and hematoxylin was used for counterstaining. Images were taken with an Olympus microscope (Olympus Corporation, Shinjuku City, Tokyo, Japan). Cytoplasmic and nuclear HDAC6 immunoreactivity were assessed semi-quantitatively on the basis of the percentage of positive cells. The cutoff value of 50% was chosen for categorization of the cytoplasmic HDAC6 expression. Nuclear HDAC6 positivity was defined as moderate-to-strong nuclear immunoreactivity in at least 40% of cells. Tissue sections underwent standardized histopathological review by the study pathologist (S-F Yang).

Cell culture and transfection

Human SK-Hep-1 cells derived from the ascitic fluid of liver adenocarcinoma were purchased from the American Type Culture Collection. Human Hep-J5, Huh-7, and Mahlavu cells were obtained from Dr. S-N Wang (KMU, Taiwan). Human Hep-G2 cells and Hep-3B cells were purchased from the Bioresource Collection and Research Center (BCRC, Hsinchu, Taiwan). The cells were cultured in the Dulbecco's modified Eagle medium (DMEM) (Gibco, Grand Island, NY, USA) containing 10% heat-inactivated fetal bovine serum (FBS, Gibco, Grand Island, NY, USA) and 100 U/mL penicillin/streptomycin at 37°C in an incubator with 5% CO_2. The cells were transfected with 50 nM of siRNA targeting HDAC6 (sc-35544, Santa Cruz Biotechnology Inc., CA, USA), HDAC6-Flag (Addgene plasmid number #13823), dominant-negative HDAC6.DC-FLAG (Addgene plasmid number #30483), or HDAC6-Nuc [12] using Lipofectamine 2000 (Invitrogen, Carlsbad, CA, USA) according to the manufacturer's instructions.

Cell proliferation assay

The cell proliferation rate was determined using the MTT colorimetric cell proliferation assay (Sigma-Aldrich, St. Louis, MO, USA). Briefly, the 5×10^3 cells were seeded in 96-well plates and incubated at 37°C to allow cell growth for 24 h. At the end of treatment, 20 μL of MTT (5 mg/mL, Sigma-Aldrich, St. Louis, MO, USA) was added to each well and the 96-well plate was incubated at 37°C in a 5% CO_2 and 95% air-humidified atmosphere for 3 h. The absorbance of the samples was dissolved with 100 μL of DMSO and measured with a spectrophotometer (Thermo Fisher Scientific, Inc.) at a wavelength of 570 nm.

Invasion assay

Cell invasion was performed using the Matrigel-coated film insert (8 μm pore size) fitted into 24-well invasion chambers (#35224; SPL Life Sciences, Pochun, South Korea). After 24 hours of incubation, the filter inserts were removed from the wells. The cells were fixed to the lower side of the insert membrane with 4% paraformaldehyde for 10 mins, followed by staining with 1% crystal violet in 2% ethanol for an additional 20 mins. The insert was then quickly merged in ddH_2O for 3-4 s to remove excess dye, and the cells on the top surface of the filter were removed using cotton swabs. The insert was dried completely, and the cell numbers were counted under an Olympus microscope (Olympus Corporation, Shinjuku City, Tokyo, Japan).

RNA extraction, Real-time PCR, and RT-PCR and RNA stability assay

Total RNA was extracted from the treated cells using Trizol reagent (Invitrogen, Carlsbad, CA, USA) according to the manufacturer instructions. The cDNA was synthesized from the total RNA using a First Strand cDNA Synthesis Kit (Thermo Fisher Scientific, Waltham, MA, USA), followed by PCR reactions containing SYBR® Select Master Mix (Applied Biosystems Inc, Foster City, CA, USA). The sequences of the primers used were shown in Table S1. The reverse transcription reaction was performed using 2 μg of total RNA and reverse transcribed into cDNA, and then, 30 cycles were amplified using oligonucleotide primers. PCR was carried out at 94°C for 30 s, at 55°C for 30 s, and at 72°C for 30 s for 32 cycles. The PCR products were subjected to 1% agarose gel electrophoresis. Quantitative data were obtained using ImageJ (National Institutes of Health, Bethesda, MD, USA). For the mRNA stability test, the cells were treated with 10 μg/ml actinomycin D for 2, 4, or 6 hours after transfection. The total RNA was then extracted. After normalization to β-actin, the group without actinomycin D treatment was considered as the baseline RNA level.

Immunoblotting analysis

Total lyses of treated cells were extracted using EBC buffer as described previously [30]. Equal amounts of the samples were separated using sodium dodecyl sulfate polyacrylamide gel electrophoresis (SDS-PAGE). The specific antibodies used were listed in Table S2.

Immunofluorescence

The cells grown on glass slides were rinsed with PBS and fixed in 4% formaldehyde at room temperature for 20 mins. The cells were washed three times with PBS and processed for indirect immunofluorescence as previously described [30]. The slides were incubated with the mouse anti-β-catenin antibody and rabbit anti-HDAC6 (sc-57535 and sc-11420, 1:400, Santa Cruz Biotechnology Inc., CA, USA). The cells were then washed and incubated with FITC-labeled goat anti-rabbit or TR-labeled goat anti-mouse (1:400, Santa Cruz Biotechnology Inc., CA, USA) antibody. Images were taken with an Olympus fluorescence microscope (U-LH100HG, Olympus Corporation, Japan).

Immunoprecipitation assay

Immunoprecipitation assay was performed according to our previous study [30]. Briefly, cell lyses were prepared in the EBC buffer. The supernatant was further incubated with mouse monoclonal antibody against HuR (sc-5261, Santa Cruz Biotechnology Inc., CA, USA). Immune complexes were precipitated with protein G-sepharose beads, followed by SDS-PAGE and Western blot assay.

Ribonucleoprotein-immunoprecipitation (RNP-IP)

The binding sites for RNA-binding proteins in human *egfr* RNA were predicted using RBPmap (http://rbpmap.technion.ac.il/index.html). RNP-IPs were performed as described [31]. Briefly, Cells were then harvested by trypsinization, and their viability was assessed by trypan blue exclusion (consistently > 95%). An equal number of cells per condition (1×10^7) was pelleted and resuspended in approximately two cell-pellet volumes of the polysome lysis buffer. The cell lysates were then frozen at -80°C for storage. At the time of use, the cell lysates were thawed and centrifuged. The cell lysate was immunoprecipitated with anti-HuR (Santa Cruz Biotechnology Inc., CA, USA). The antibody-coated beads were extracted using phenol-chlorophorm-isoamylalcohol and precipitation in ethanol. The isolated RNA was subjected to RT-qPCR analysis, as described above.

Statistical analysis

Statistical analyses were performed using SPSS 26.0 (SPSS, Chicago) software. Groups of patients with different subcellular HDAC6 distributions were correlated with clinicopathological characteristics using the chi-square method. All statistical tests were two-sided. $P < 0.05$ was considered statistically significant. The results are expressed as means ± SEM.

Results

Increased levels of HDAC6 were positively correlated with a poor prognosis and worse survival in HCC patients

To investigate the clinical role of subcellular expression of HDAC6 in liver cancer, IHC was first performed on tissue microarrays (n = 122). The staining results of HDAC6 in liver cancer tissues are shown in Fig. 1a. Both cytoplasmic and nuclear HDAC6 expressions mainly decreased in HCC tissues (65.6% and 63.9%, respectively). Furthermore, the increased cytoplasmic HDAC6 staining was positively correlated with recurrence rate (Table 1; $p = 0.002$) and with poor patient survival (Fig. 1b; $p = 0.038$). No significant correlation between nuclear HDAC6 staining and any pathological characteristic was found in our cases. However, an increased nuclear HDAC6 frequency was associated with a poor outcome in HCC patients (Fig. 1b; $p = 0.002$). Taken together, increased levels of HDAC6 might contribute to poor prognosis and survival of liver cancer and might promote advanced development through distinct subcellular localization.

HDAC6 promoted the proliferation and invasion of liver cancer cells

HDAC6 protein was expressed in Hep-G2, Hep-3B, and SK-Hep-1 cells, but was not detected in Hep-J5, Huh-7, and Mahlavu cells, as shown in Fig. 2a. In HDAC6-expressing Hep-G2, Hep-3B, and SK-Hep-1 cells, HDAC6 was mainly located in the cytoplasm (Fig. 2b). Although increased cytoplasmic HDAC6 was positively correlated with recurrence rate (Table 1) and with poor patient survival (Fig. 1b), the invasion activity was not in parallel with the expression of HDAC6 in those liver cancer cells (Fig. 2c). To further explore the potential roles of HDAC6 in liver cancer, a gain-of-function study was performed first in Hep-J5, Huh-7, and Mahlavu cells, which have undetectable HDAC6 proteins. The ectopic overexpression of HDAC6-Flag enhanced cell proliferation in Hep-J5, Huh-7, and Mahlavu cells (Fig. 3a). In addition, the invasion rate of cells transiently transfected with wild-type HDAC6-Flag was significantly higher than that of the control: Hep-J5, Huh-7, and Mahlavu cells (Fig. 3b). Intriguingly, the ectopic overexpression of HDAC6-Flag increased the activation of AKT in Hep-J5, Huh-7, and Mahlavu cells (Fig. 3c). Accordingly, the restoration of HDAC6 proteins in Hep-J5, Huh-7, and Mahlavu cells promoted the

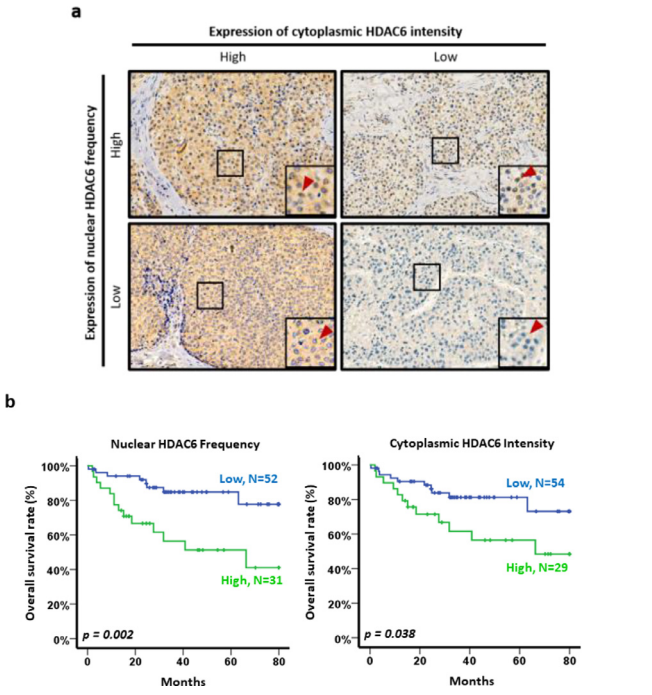

Fig. 1. The association between different subcellular localization of HDAC6 and survival in a patient with HCC. (a) The IHC results show the expression of HDAC6 in the HCC tissues, original magnification, 400X. (b) HCC patients with increased nuclear frequency or cytoplasmic intensity of HDAC6 have poor overall survival rates.

entry of β-catenin into the nucleus (Fig. 3d-f). An increased frequency of nuclear HDAC6 was associated with a poor outcome in liver cancer patients (Fig. 1b). It is noted that the increased deacetylation of p53 at lysine K120 is able to activate apoptosis [32,33]. We found that both HDAC6-Flag and, in particular, HDAC6-Nuc facilitated the deacetylation of p53 at lysine K120 in Hep-J5, Huh-7, and Mahlavu cells (Fig. 3g). In short, increased levels of HDAC6 promoted the proliferation and invasion of liver cancer cells through the deacetylation of tumor suppressor p53 and increased AKT/β-catenin signaling.

Ectopic overexpression of HDAC6 restored EGFR expression

A positive correlation between HDAC6 and EGFR proteins was found in several liver cancer cell lines (Fig. 2a), and HDAC6 was able to activate AKT/β-catenin signaling in liver cancer cells (Fig. 3). Intriguingly, the restoration of wild-type, HDAC6-Flag or dominant (deacetylase)-negative mutant, HDAC6.DC-FLAG but not nuclear localized only, HDAC6-Nuc in Hep-J5, Huh-7, and Mahlavu cells increased the levels of EGFR proteins (Fig. 4a). The knockdown of HDAC6 with specific siRNA decreased the expression of EGFR proteins in Hep-G2, Hep- 3B, and SK-Hep-1 cells (Fig. 4b). EGFR-specific siRNA slightly decreased the expression of HDAC6 in SK-Hep-1 cells (Fig. 4c), while HDAC6- and EGFR-specific siRNA decreased both proliferation (Fig. 4d) and invasion (Fig. 4e) in SK-Hep-1 cells. The HDAC6-restored EGFR expression was abrogated by EGFR-specific siRNA in HDAC6-transfected Hep-J5, Huh-7, and Mahlavu cells (Fig. 4f). Accordingly, the proliferation and invasive ability of Hep-J5, Huh-7, and Mahlavu cells induced by HDAC6 were significantly attenuated by knockdown of EGFR (Fig. 4g-h). These results suggested that the HDAC6-mediated EGFR expression contributed to both proliferation and invasion induced by HDAC6 in liver cancer cells.

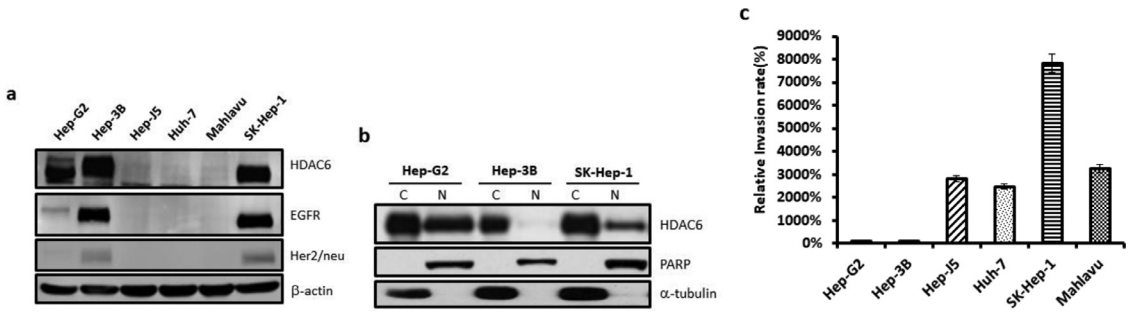

Fig. 2. HDAC6 is correlated with EGFR overexpression in human liver cell lines and patient specimens. (a) Expressions of HDAC6, EGFR, and ERBB2 in the liver cell lines Hep-G2, Hep-3B, Hep-J5, Huh-7, SK-Hep-1, and Mahlavu detected using Western blot analysis. (b) Cytoplasmic (C) and nuclear (N) fractions were subjected to immunoblot analysis with the indicated antibodies. (c) Invasion of Hep-G2, Hep-3B, Hep-J5, Huh-7, SK-Hep-1, and Mahlavu cells was measured using Trans well assays (mean ± SEM, $^{*}p < 0.01$).

Table 1

The correlation of HDAC6 intensity and frequency with clinicopathological characteristics in liver cancer tissues.

Characteristics	N	Intensity of HDAC6		*p* value	Frequency of HDAC6		*p* value
		Low (n = 80)	High (n = 42)		Low (n = 78)	High (n = 44)	
Years				0.214			0.086
≦ 60	76 (62.3%)	53	23		53	23	
> 60	46 (37.7%)	27	19		25	21	
Gender				0.405			0.870
Female	35 (28.7%)	14	10		15	9	
Male	87 (71.3%)	66	32		63	35	
Viral marker				0.904			0.181
HBV (-)/HCV (-)	9 (10.9%)	6	3		5	4	
HBV (+)/HCV (-)	44 (53.0%)	30	14		32	12	
HBV (-)/HCV (+)	22 (26.5%)	13	9		10	12	
HBV (+)/HCV (+)	8 (9.6%)	5	3		5	3	
Histological grade				0.304			0.341
I	14 (16.9%)	11	3		11	3	
II	57 (68.7%)	34	23		33	24	
III	12 (14.5%)	9	3		8	4	
Tumor stage				0.270			0.299
I	30 (25.0%)	20	10		22	8	
II	58 (48.4%)	39	19		37	21	
III	28 (23.3%)	15	13		14	14	
IV	4 (3.4%)	4	0		3	1	
Recurrence				0.002*			0.088
Absent	50 (60.2%)	39	11		35	16	
Present	33 (39.8%)	15	18		17	16	

NOTE. Data are determined by Chi-square Tests. Abbreviations: HCV, anti-hepatitis C virus antibody; HBV, hepatitis B surface antigen; (+), positive or present; (-), negative or absent

HDAC6 stabilized egfr mRNA in liver cancer cells

Upon further examining if the HDAC6-induced EGFR expression was mediated at post-translation levels (i.e., protein stability), the cells were treated with a reversible proteasome inhibitor MG132 (proteasome inhibitor, 5 μM) for 6 h after transfection for 24 h. The expression of EGFR protein was not affected by treatment with MG132 in Hep-J5, Huh-7, and Mahlavu cells. In addition, ectopic HDAC6 overexpression in combination with MG132 did not increase the expression of EGFR in Hep-J5, Huh-7, and Mahlavu cells (Fig. 5a). The increased levels of mRNA in accordance with the increased protein levels might be due to the increased mRNA stability or transcription activity. An intriguing report has showed that decreased levels of HDAC6 result in *erbb2* mRNA destabilization [16]. The UCSC Xena browser (https://xenabrowser.net) showed that the expression levels of *erbb2* mRNA were indeed positively correlated with those of *hdac6* mRNA (Fig. 5b; $p < 0.001$). Similarly, the expression levels of *egfr* mRNA were also positively correlated with those of *hdac6* mRNA (Fig. 5b; $p < 0.001$). The ligand-independent expression of EGFR protein and mRNA was dramatically increased upon the restoration of HDAC6 in Hep-J5, Huh-7, and Mahlavu cells (Fig 5a and 5c). Furthermore, wild-type HDAC6 increased the stability of *egfr* mRNA compared with the control in Hep-J5, Huh-7, and Mahlavu cells when treated with actinomycin D (Fig. 5c). These results demonstrated that the HDAC6-mediated ligand- and deacetylase-independent increase in EGFR protein was mediated by the enhanced stability of *egfr* mRNA.

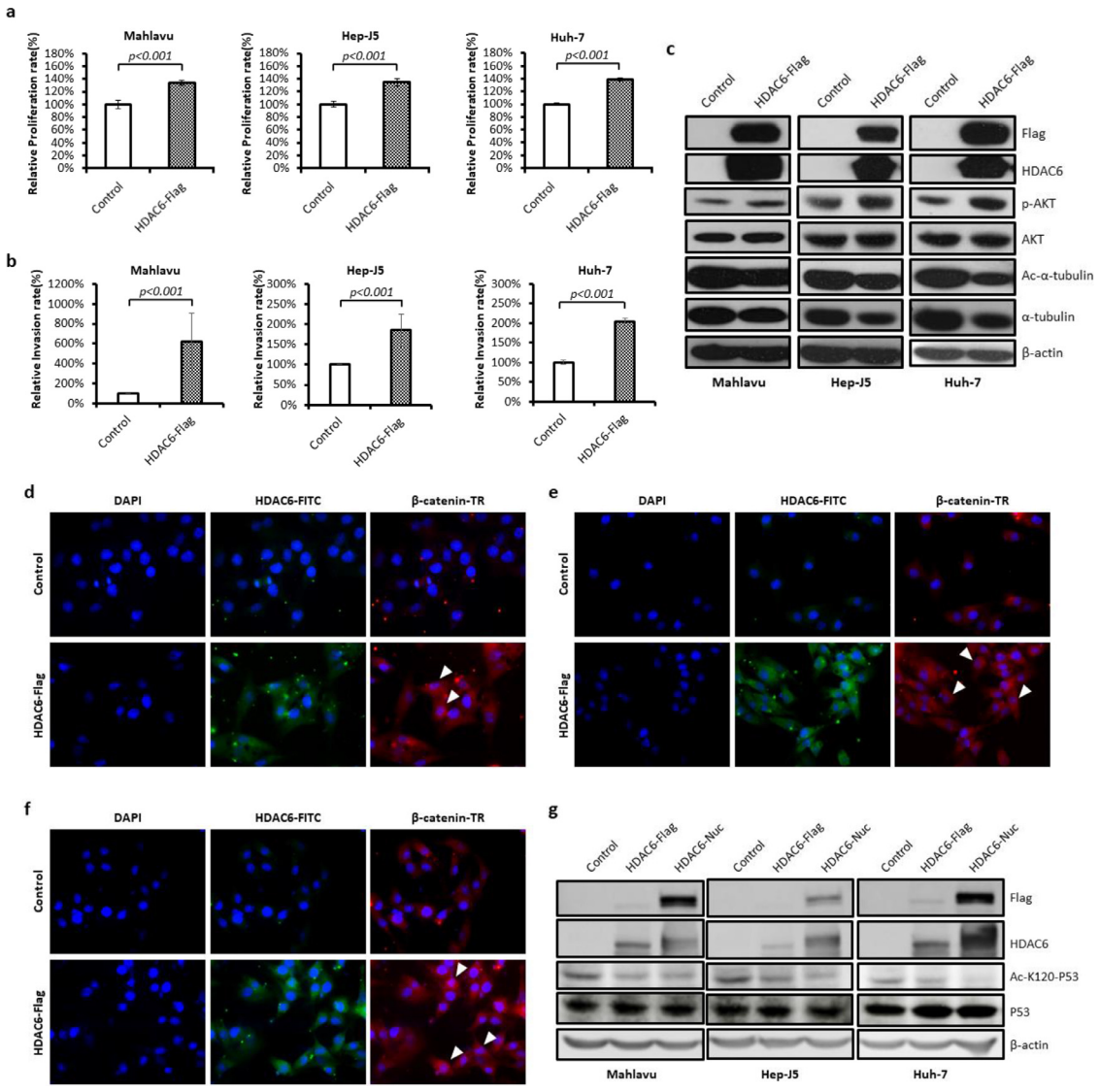

Fig. 3. HDAC6 promoted proliferation and invasion of liver cancer cells. Ectopic overexpression of HDAC6 increased cell (a) proliferation and (b) invasion rate of Hep-J5, Huh-7, and Mahlavu cells. (c) Ectopic overexpression of HDAC6 activated AKT signaling in HCC cells. (d-f) Immunofluorescent staining showed that the ectopic overexpression of HDAC6 protein (FITC; green) increased the levels of β-catenin protein (Texas- Red) and promoted the trans-localization of β-catenin protein into the nuclei of Hep-J5, Huh-7, and Mahlavu cells. (g) Cells were transfected as indicated and the levels of the FLAG-tagged proteins, p53, Ac-p53 (K120), and β-actin were detected by Western blotting.

HDAC6 bound to the 3′ UTR of egfr mRNA in liver cancer cells

Our results showed that HDAC6 immunoprecipitates were indeed enriched with HuR (Fig. 5d). To determine whether HuR binds directly to *egfr* mRNA in liver cancer cells, an RNP-IP assay was performed on lysates prepared from the Mahlavu cells transfected with or without HDAC6 expression plasmid for 24 h. An RNP-IP with a HuR-specific antibody was used to isolate total mRNA transcripts associated with HuR, followed by qPCR to determine the amount of HuR protein-associated 3′UTR of the *egfr* mRNA. Ectopic HDAC6 overexpression significantly increased the specific HuR binding to the 3′UTR of *egfr* mRNA to six times compared with un-transfected cells (Fig. 5e). These results indicated that HDAC6 enhanced the aggressive behaviors of liver cancer cells by enhancing the HuR-mediated mRNA stability of *egfr* mRNA, leading to increased EGFR expression and related signaling. In summary, our data indicate that the HDAC6-EGFR axis might be involved in the development of advanced liver cancer.

Discussion

Curing HCC is very challenging due to the lack of a full understanding of HCC recurrence. Even now, the precise molecular mechanisms that account for this phenomenon remain unclear. HDAC6 has been shown to contribute to tumorigenesis in several types of human cancers and to function as a key regulator of many cancer biological processes [34–37]. In this study, our results revealed that cytoplasmic HDAC6 was positively correlated with recurrence and poor survival of liver cancer patients. The ectopic expression of HDAC6 induced the proliferation and invasion of liver cancer cells, which might have resulted from the HDAC6-associated improvement in *egfr* mRNA stability and subsequently activated p-AKT/β-catenin signaling pathway. Importantly, the HDAC6-EGFR axis might increase ligand-independent activation of AKT and the accumulation of nuclear β-catenin, leading to the development of advanced liver cancer. Indeed, the expression levels of HDAC6 and EGFR proteins were positively

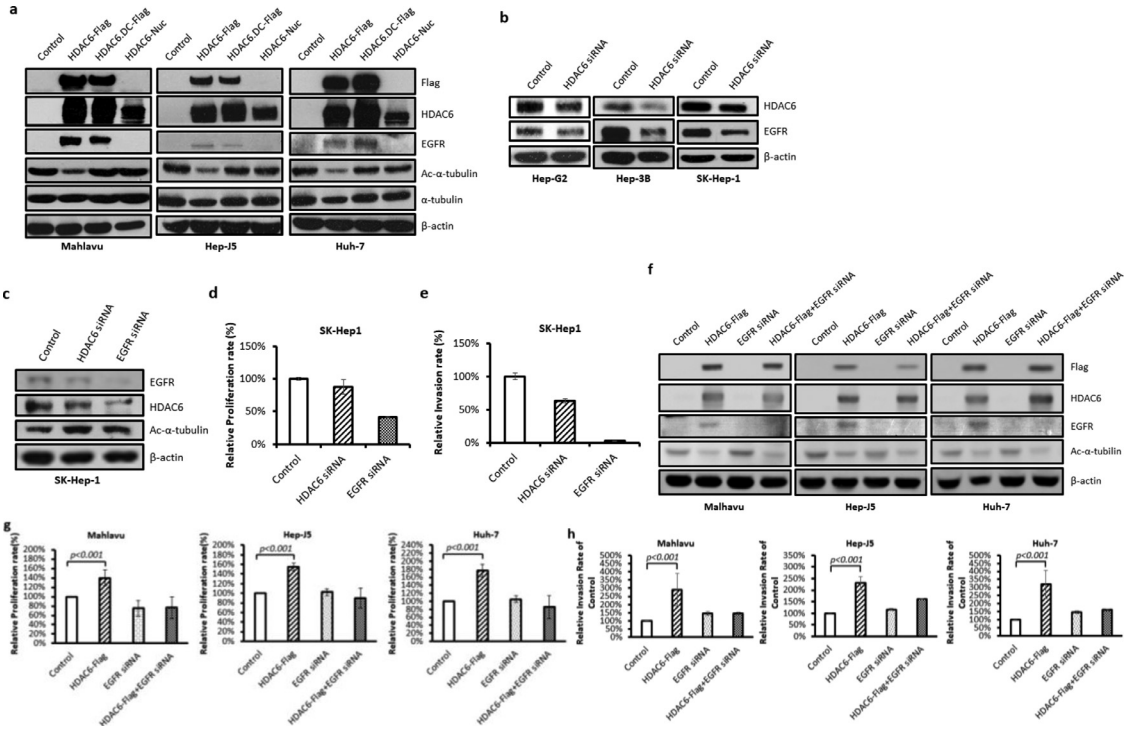

Fig. 4. HDAC6 controls EGFR expression in liver cancer cells. (a) Cells were transfected as indicated and EGFR protein level was detected by Western blot. Wild-type HDAC6: HDAC6-Flag; catalytically inactive mutant (H216/611A): HDAC6.DC-FLAG; NES-deleted HDAC6: HDAC6-Nuc. (b) Knockdown of HDAC6 with specific siRNA decreased the expression of EGFR in Hep-G2, Hep-3B, and SK-Hep1 cells. Transient transfection with siRNA targeting HDAC6 or EGFR (c) significantly reduced (d) cell proliferation and (e) invasion in SK-Hep-1 cells, respectively. (f) EGFR-specific siRNA could reverse the HDAC6-induced EGFR protein expression, (g) cell proliferation, and (h) invasion, respectively.

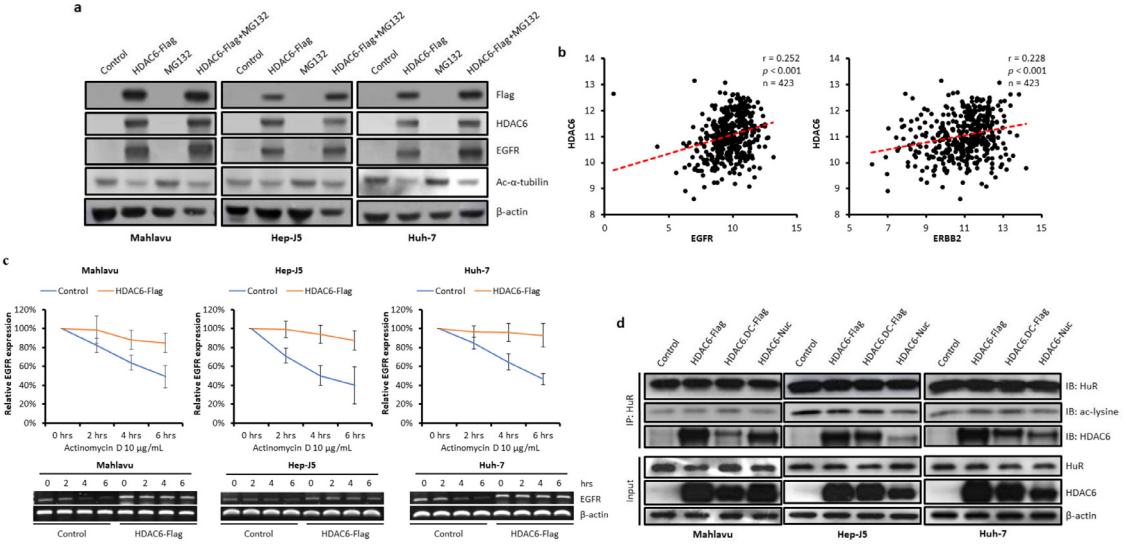

Fig. 5. Changes in HDAC6 levels affect expression of *egfr* mRNA. (a) MG132 treatment (5 μM, 6 h) did not reverse the expressions of HDAC6 and EGFR in Hep-J5, Huh-7, and Mahlavu cells. (b) Correlation between *hdac6, egfr*, and *erbb2* mRNA expression in the TCGA database, identified using UCSC Xena. (c) Hep-J5, Huh-7, and Mahlavu cells transfected with either HDAC6-Flag or HDAC6.DC-FLAG were treated with actinomycin D for different durations, and the mRNA levels of *egfr* were measured by RT-PCR. (d) The interaction between HDAC6 and HuR was analyzed by immunopreciptation using the antibody against HuR in HDAC6-Flag, HDAC6.DC-FLAG, and HDAC6-Nuc-transfected liver cancer cells. (e) RNP-IP assays showing increased binding of *egfr* mRNA to HuR in response to HDAC6 expression level. HuR-protein-bound *egfr* mRNA amounts in Mahlavu cells grown for 24 h, measured by qPCR. .

correlated in liver cancer cell lines, while their transcripts were also positively correlated with the liver cancer tissues. Intriguingly, ectopic overexpression of HDAC6-Flag increased the levels of EGFR proteins in Hep-J5, Huh-7, and Mahlavu cells. Additionally, the knockdown of HDAC6 with specific siRNA decreased the expression of EGFR proteins in Hep-G2, Hep-3B, and SK-Hep-1 cells. We believed that these effects of HDAC6 on EGFR expression mainly depended on the function of cytoplasmic HDAC6 because a nuclear HDAC6 mutant could not restore EGFR expression in three liver cancer cells. Importantly, our results showed that the HDAC6-restored EGFR expression was abrogated by EGFR-specific siRNA in HDAC6-transfected Hep-J5, Huh7, and Mahlavu cells. Accordingly, the proliferation and invasive abilities of Hep-J5, Huh-7, and Mahlavu cells induced by HDAC6 were significantly attenuated by the knockdown of EGFR. These results suggest that the HDAC6-mediated EGFR expression contributed to both proliferation and invasion induced by HDAC6 in liver cancer cells. The HDAC6-EGFR axis could promote the development of advanced liver cancer and might serve as a druggable target in liver cancer.

Further analysis showed that HDAC6-induced EGFR expression was mediated through increasing mRNA stability. HDAC6 played a key role in promoting EGFR expression by indirectly binding to its 3′UTR at the post-transcriptional level. In addition, HuR bound to the 3′UTR of *egfr* mRNA in a HDAC6-dependent manner. The HDAC6-mediated increase in mRNA levels was unaffected by treatment with actinomycin D, confirming that HDAC6 enhanced the transcript stability of *egfr* mRNA. HDAC6 has been reported to be associated with HuR in an RNA-dependent interaction or to be tethered by an unknown RNA-binding protein to the 3′UTR [16]. Our results revealed that HDAC6 showed an up to 4-8-fold increase in the levels of ARE bearing *egfr* mRNA, whereas mutated HDAC6 showed a decreased effect. Consistently, the knockdown of HDAC6 is not functionally equivalent to catalytic inhibition of its deacetylase activity, and α-tubulin acetylation does not functionally correlate with *erbb2* mRNA destabilization [16]. In addition, HuR expression strongly stabilizes HuR-regulated transcripts such as SOX9, VEGFA, and EGFR [15]. Our findings showed for the first time that HDAC6 could increase the ligand- and deacetylase-independent expressions of EGFR proteins in liver cancer cells. This phenomenon is not the same as those reported in other studies [18,42,43]. The pharmacologic inhibition of HDAC6 regulates endocytic trafficking and the degradation of EGFR proteins through the modulation of tubulin acetylation [18], while the knockdown of HDAC6 leads to the deregulation of microtubule-dependent endocytic vesicle trafficking and accelerates EGFR degradation [18,42,43].

In this study, the increased nuclear HDAC6 frequency was associated with a poor outcome in HCC patients. HDAC6 has been reported to deacetylate p53 at K120, which is required for p53-induced apoptosis in tumors [38,39], implying that the associations between nuclear HDAC6 and poor outcome might be due to the potential deacetylation of p53 in liver cancer. As shown in Fig. 3g, both HDAC6-Flag and, in particular, HDAC6-Nuc facilitated the deacetylation of p53 at lysine K120 in Hep-J5, Huh-7, and Mahlavu cells. Previous studies from other groups provide *in vitro* evidence demonstrating that HDAC6 plays a role in HCC development through the regulation of p53 protein stability [5]. Additionally, HDAC6 is able to bind to the lysine residue of p53 via its deacetylase domain [40,41]. Notably, the knockdown of HDAC6 with specific siRNA decreased the expression of EGFR on Hep-G2 (p53-wt), Hep-3B (p53-null), and SK-Hep-1 (p53-wt), suggesting that HDAC6-mediated EGFR expression was a p53-independent manner. Taken together, increased levels of HDAC6 might contribute to poor prognosis and the survival of liver cancer cells and might promote the development of advanced liver cancer through the deacetylation of tumor suppressor p53 (i.e., nuclear HDAC6) and increased AKT/β-catenin signaling (i.e., cytoplasmic HDAC6).

Altogether, our findings reveal an important role for different subcellular locations of HDAC6 in the control of liver cancer development via upregulating EGFR-mediated AKT/β-catenin signaling and deacetylated p53 at K120, suggesting that an alteration in HDAC6 expression and/or activity may be an important event in the development of aggressive liver cancer. HDAC6 is able to improve *egfr* mRNA stability through its interaction with HuR in ligand-, deacetylase-, and p53-independent manners. The HDAC6-EGFR axis may be a critical and key player in liver cancer and may serve as a druggable target in the future.

Declaration of Competing Interest

The authors declare that they have no conflict of interest.

CRediT authorship contribution statement

Hong-Ying Dai: Methodology, Validation, Investigation, Visualization, Writing – original draft. **Long-Sen Chang:** Methodology, Investigation, Supervision, Writing – review & editing. **Sheau-Fang Yang:** Formal analysis, Data curation, Writing – review & editing. **Shen-Nien Wang:** Data curation, Resources, Writing – review & editing. **Shu-Jem Su:** Data curation, Writing – review & editing. **Yao-Tsung Yeh:** Conceptualization, Data curation, Writing – original draft, Writing – review & editing, Visualization, Supervision, Project administration.

Acknowledgments

This study was supported, in part, by grants from the Ministry of Science and Technology, Taiwan (MOST 105-2320-B-242-002-MY3).

Supplementary materials

Supplementary material associated with this article can be found, in the online version, at doi:10.1016/j.neo.2022.100845.

Reference

[1] Li, G., Y. Tian, and W.-G. Zhu, The Roles of Histone Deacetylases and Their Inhibitors in Cancer Therapy. 2020. 8.

[2] Li Y, Shin D, Kwon SH. Histone deacetylase 6 plays a role as a distinct regulator of diverse cellular processes. *Febs j* 2013;**280**(3):775–93.

[3] Zhang Y, et al. Two catalytic domains are required for protein deacetylation. *J Biol Chem* 2006;**281**(5):2401–4.

[4] Li T, et al. Histone deacetylase 6 in cancer. *Journal of Hematology & Oncology* 2018;**11**(1):111.

[5] Ding G, et al. HDAC6 promotes hepatocellular carcinoma progression by inhibiting P53 transcriptional activity. *FEBS Lett* 2013;**587**(7):880–6.

[6] Kanno K, et al. Overexpression of histone deacetylase 6 contributes to accelerated migration and invasion activity of hepatocellular carcinoma cells. *Oncol Rep* 2012;**28**(3):867–73.

[7] Yang HD, et al. HDAC6 Suppresses Let-7i-5p to Elicit TSP1/CD47-Mediated Anti-Tumorigenesis and Phagocytosis of Hepatocellular Carcinoma. *Hepatology* 2019;**70**(4):1262–79.

[8] Jung KH, et al. Histone deacetylase 6 functions as a tumor suppressor by activating c-Jun NH2-terminal kinase-mediated beclin 1-dependent autophagic cell death in liver cancer. *Hepatology* 2012;**56**(2):644–57.

[9] Hubbert C, et al. HDAC6 is a microtubule-associated deacetylase. *Nature* 2002;**417**(6887):455–8.

[10] Matsuyama A, et al. In vivo destabilization of dynamic microtubules by HDAC6-mediated deacetylation. *EMBO J* 2002;**21**(24):6820–31.

[11] Riolo MT, et al. Histone deacetylase 6 (HDAC6) deacetylates survivin for its nuclear export in breast cancer. *J Biol Chem* 2012;**287**(14):10885–93.

[12] Yang CJ, et al. Nuclear HDAC6 inhibits invasion by suppressing NF-κB/MMP2 and is inversely correlated with metastasis of non-small cell lung cancer. *Oncotarget* 2015;**6**(30):30263–76.

[13] Guillemin, A., et al., Shaping the Innate Immune Response Through Post-Transcriptional Regulation of Gene Expression Mediated by RNA-Binding Proteins. Front Immunol, 2021. 12: p. 796012.

[14] Schultz CW, et al. Understanding and targeting the disease-related RNA binding protein human antigen R (HuR). *Wiley Interdiscip Rev RNA* 2020;**11**(3):e1581.

[15] Sharma S, et al. The interplay of HuR and miR-3134 in regulation of AU rich transcriptome. *RNA Biol* 2013;**10**(8):1283–90.

[16] Scott GK, et al. Destabilization of ERBB2 transcripts by targeting 3′ untranslated region messenger RNA associated HuR and histone deacetylase-6. *Mol Cancer Res* 2008;**6**(7):1250–8.

[17] Wang Z, et al. HDAC6 promotes cell proliferation and confers resistance to gefitinib in lung adenocarcinoma. *Oncol Rep* 2016;**36**(1):589–97.

[18] Liu W, et al. HDAC6 regulates epidermal growth factor receptor (EGFR) endocytic trafficking and degradation in renal epithelial cells. *PLoS One* 2012;**7**(11):e49418.

[19] Gao YS, Hubbert CC, Yao TP. The microtubule-associated histone deacetylase 6 (HDAC6) regulates epidermal growth factor receptor (EGFR) endocytic trafficking and degradation. *J Biol Chem* 2010;**285**(15):11219–26.

[20] Berasain C, Avila MA. The EGFR signalling system in the liver: from hepatoprotection to hepatocarcinogenesis. *J Gastroenterol* 2014;**49**(1):9–23.

[21] Huether A, et al. Erlotinib induces cell cycle arrest and apoptosis in hepatocellular cancer cells and enhances chemosensitivity towards cytostatics. *J Hepatol* 2005;**43**(4):661–9.

[22] Buckley AF, et al. Epidermal growth factor receptor expression and gene copy number in conventional hepatocellular carcinoma. *Am J Clin Pathol* 2008;**129**(2):245–51.

[23] Sueangoen N, Tantiwetrueangdet A, Panvichian R. HCC-derived EGFR mutants are functioning, EGF-dependent, and erlotinib-resistant. *Cell & Bioscience* 2020;**10**(1):41.

[24] Xia H, et al. EGFR-PI3K-PDK1 pathway regulates YAP signaling in hepatocellular carcinoma: the mechanism and its implications in targeted therapy. *Cell Death Dis* 2018;**9**(3):269.

[25] Rimassa L, et al. Management of adverse events associated with tyrosine kinase inhibitors: Improving outcomes for patients with hepatocellular carcinoma. *Cancer Treat Rev* 2019;**77**:20–8.

[26] Zhao D, et al. Upregulation of HIF-2α induced by sorafenib contributes to the resistance by activating the TGF-α/EGFR pathway in hepatocellular carcinoma cells. *Cell Signal* 2014;**26**(5):1030–9.

[27] Jin H, et al. EGFR activation limits the response of liver cancer to lenvatinib. *Nature* 2021;**595**(7869):730–4.

[28] Edge SB, Compton CC. The American Joint Committee on Cancer: the 7th edition of the AJCC cancer staging manual and the future of TNM. *Ann Surg Oncol,* 2010;**17**(6):1471–4.

[29] Yang SF, et al. Altered p-STAT3 (tyr705) expression is associated with histological grading and intratumour microvessel density in hepatocellular carcinoma. *J Clin Pathol* 2007;**60**(6):642–8.

[30] Yang SF, et al. Increased caveolin-1 expression associated with prolonged overall survival rate in hepatocellular carcinoma. *Pathology* 2010;**42**(5):438–45.

[31] Hassan MQ, et al. Ribonucleoprotein immunoprecipitation (RNP-IP): a direct in vivo analysis of microRNA-targets. *J Cell Biochem* 2010;**110**(4):817–22.

[32] Tang Y, et al. Tip60-dependent acetylation of p53 modulates the decision between cell-cycle arrest and apoptosis. *Mol Cell* 2006;**24**(6):827–39.

[33] Yoo J, et al. HDAC6-selective inhibitors enhance anticancer effects of paclitaxel in ovarian cancer cells. *Oncol Lett* 2021;**21**(3):201.

[34] Park SJ, et al. HDAC6 sustains growth stimulation by prolonging the activation of EGF receptor through the inhibition of rabaptin-5-mediated early endosome fusion in gastric cancer. *Cancer Lett* 2014;**354**(1):97–106.

[35] Gradilone SA, et al. HDAC6 inhibition restores ciliary expression and decreases tumor growth. *Cancer Res* 2013;**73**(7):2259–70.

[36] Aldana-Masangkay GI, Sakamoto KM. The role of HDAC6 in cancer. *J Biomed Biotechnol* 2011;**2011**:875824.

[37] Li S, et al. Histone deacetylase 6 promotes growth of glioblastoma through inhibition of SMAD2 signaling. *Tumour Biol* 2015;**36**(12):9661–5.

[38] Sen N, et al. HDAC5, a key component in temporal regulation of p53-mediated transactivation in response to genotoxic stress. *Mol Cell* 2013;**52**(3):406–20.

[39] Bitler BG, et al. ARID1A-mutated ovarian cancers depend on HDAC6 activity. *Nat Cell Biol* 2017;**19**(8):962–73.

[40] Ryu HW, et al. HDAC6 deacetylates p53 at lysines 381/382 and differentially coordinates p53-induced apoptosis. *Cancer Lett* 2017;**391**:162–71.

[41] Park SY, et al. HDAC6 deficiency induces apoptosis in mesenchymal stem cells through p53 K120 acetylation. *Biochem Biophys Res Commun* 2017;**494**(1-2):51–6.

[42] Gu YZ, et al. Different roles of PD-L1 and FasL in immunomodulation mediated by human placenta-derived mesenchymal stem cells. *Hum Immunol* 2013;**74**(3):267–76.

[43] Wen J, et al. MIIP accelerates epidermal growth factor receptor protein turnover and attenuates proliferation in non-small cell lung cancer. *Oncotarget* 2016;**7**(8):9118–34.